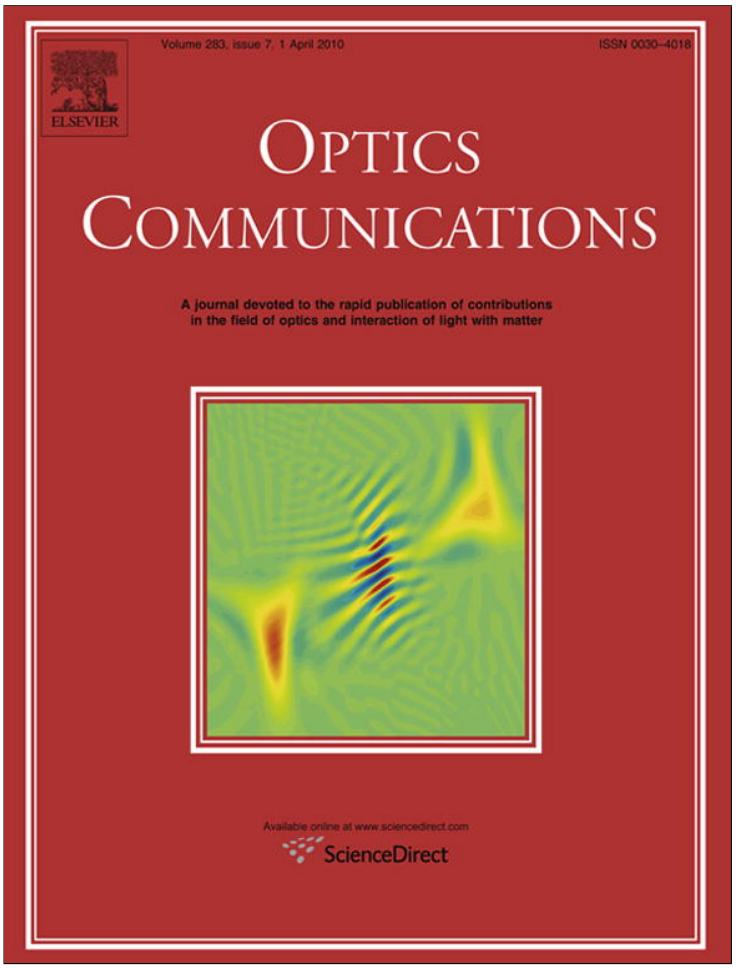

Optics Communications 283 (2010) 1476–1480

Contents lists available at ScienceDirect

Optics Communications

journal homepage: www.elsevier.com/locate/optcom

Generation of quadratic spatial dark soliton in periodically poled lithium niobate

Yong Yang, Yi Yang, Xianfeng Chen *

Department of Physics, The State Key Laboratory on Fiber Optic Local Area Communication Networks and Advanced Optical Communication Systems, Shanghai Jiao Tong University, 800, Dong Chuan Road, Shanghai 200240, China

ARTICLE INFO

Article history:
Received 25 June 2009
Received in revised form 14 October 2009
Accepted 24 November 2009

Keywords:
Dark spatial soliton
Cascaded quadratic nonlinearity

ABSTRACT

In this paper, we report the evolution of quadratic spatial dark soliton in periodically poled lithium niobate (PPLN). The generation of solitons pairs by wavefront modulation methods is investigated in both numerical simulations and experiments. We found that quadratic dark spatial solitons have analogue performances compared with that in $\chi^{(3)}$ defocusing Kerr media.

Spatial optics solitons has attracted much research interests because its physics essence and potential applications in all-optical devices [1–10]. The theory of dark soliton solution was first discovered by Zakharov and Shabat using the inverse scattering method [11]. Experimentally, Kerr solitons have been observed in CS_2, glass, semiconductor, and polymer waveguides [12]. More recently, attention has been paid to soliton formation by use of cascaded second-order nonlinearities in quadratic (χ^2) media. The large nonlinear phase shift in fundamental wave during SHG was first discussed by Ostrovskii [13] and the existence of solitons was predicted in 1974 by Karamzin and Sukhorukov [14]. In the past decades, it has been already proved experimentally that bright solitary waves can exist with the cascaded second-order nonlinearities ($\chi^{(2)}$:$\chi^{(2)}$) in quadratic media [15–19]. Advanced study on cascading effect and the induced Kerr effect was conducted by Bang et al. Theoretically, Bang and his colleagues showed that quadratic solitons are equivalent to solitons of a nonlocal Kerr medium [20–24]. Assanto and Stegeman used the concepts of cascading phase shift to interpret the formation and properties of quadratic solitons [25]. Bright spatial solitons have been observed in periodically poled $LiNbO_3$ and $KTiOPO_4$ due to cascaded second-order nonlinearities [26,27]. Because both positive and negative values of n_2^{cascad} are observed and measured in Quasi-phase-matched (QPM) cascaded SHG process [28], It is expected that dark solitons by $\chi^{(2)}$:$\chi^{(2)}$ nonlinearity in QPM configuration can be observed.

In this *Letter*, we report theoretically and experimentally the dark spatial soliton pairs generated by wavefront modulation method in QPM cascaded SHG process. By using a metal wire or a phase retard plate, single spatial soliton or soliton pairs are observed.

Under the condition of slowly varying envelope approximation, we get the wave-coupling equations of spatial soliton in a quasi-phase-matched (QPM) quadratic nonlinearity media. They used to be reduced in normalized form,

$$\begin{aligned} &i\tfrac{\partial a_1}{\partial \xi} + \tfrac{1}{2}\nabla_\perp^2 a_1 + d(\xi)a_1^* a_2 \exp(-i\beta\xi) = 0 \\ &i\tfrac{\partial a_2}{\partial \xi} + \tfrac{\alpha}{2}\nabla_\perp^2 a_2 - i\delta\nabla_\perp^2 a_2 + d(\xi)a_1^2 \exp(i\beta\xi) = 0 \end{aligned}, \tag{1}$$

where a_1, a_2 are the normalized amplitudes of the fundamental and harmonic waves, respectively, $\alpha = \frac{k_1}{k_2}$, k_1, k_2 are the wave numbers at the two frequencies. The parameter β ($\beta = k_1\eta^2\Delta k$) is proportional to the phase mismatch Δk ($\Delta k = 2k_1 - k_2 + \frac{2\pi}{\Lambda}$, Λ is the one-order quasi-phase-matched grating period) and η is the characteristic beam transverse width. ξ is the propagation distance in the unit of $k_1\eta^2$. δ accounts for the Poynting vector walk-off when propagation is not along the crystal optical axes. We can set $\delta = 0$ because Poynting vector walk-off is absent in typical QPM geometries. The function $d(\xi)$ stands for the effective nonlinear coefficients involved in QPM. $\nabla_\perp$ represents $\delta/\delta s$ in the situation of one dimension, here s is the normalized transverse coordinate in the unit of η.

Based on the above wave-coupling equation, the generation and evolution of dark solitons under various conditions can be numerically simulated [29] with a split-step approach. In split-step method, firstly the diffraction effects are calculated by Fourier integral. Secondly nonlinear effects are calculated by Runge–Kutta method. In Kerr media, it has been observed experimentally that the beam splitting occurs after a certain value of the input beam intensity has been reached. The dark solitons are evolved and generated in pairs [30]. The nth pair from the center of the beam is called nth-order pair. These phenomena result from the inherent

* Corresponding author. Tel.: +86 21 54743252; fax: +86 21 54741040.
E-mail address: xfchen@sjtu.edu.cn (X. Chen).

0030-4018/$ - see front matter © 2009 Elsevier B.V. All rights reserved.
doi:10.1016/j.optcom.2009.11.067

repulsive character of their interaction: it is energetically favorable to break a soliton into two pieces traveling away from each other. Naturally, a problem is raised: does the optical branching effect occur in the cascaded quadratic media? Box-like dark spatial pulse as an initial input condition is suitable for analyzing the branching effect. An ideal box-like pulse is given by:

$$\begin{cases} A = 0 & |x| < a \\ A = 1 & |x| > a \end{cases} \tag{2}$$

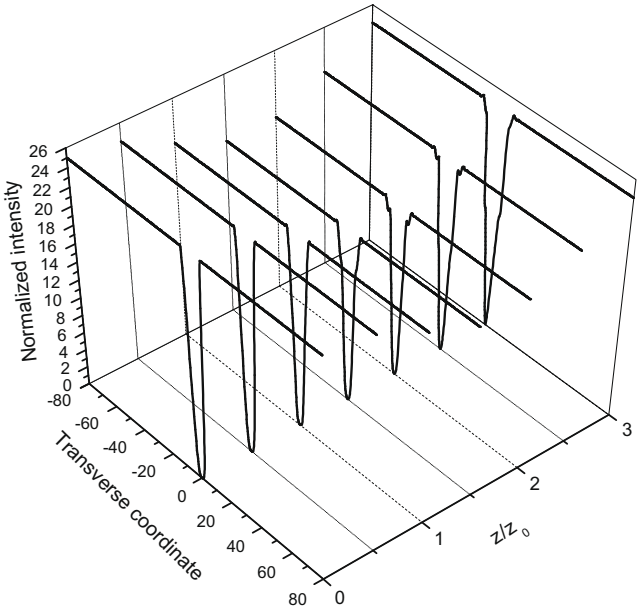

Fig. 1. The transfer process of dark soliton. $A = 5$, $\beta = -15$, the propagation distance z is varied from 0 to $3Z_0$.

If above ideal box-like pulse is employed as initial condition, the simulation results are singular due to abrupt discontinuity at the points $x = \pm a$. In order to avoid this issue, an input beam described by function below is introduced to simulate the box-like dark solitons:

$$\begin{cases} A\exp\left[-\frac{(x+400)^2}{400}\right] & -500 < x < -400 \\ A & -400 < x < -b\pi \\ \frac{A}{2}\left[\cos\left(\frac{x}{b}+\pi\right)+1\right] & -b\pi < x < b\pi \\ A & b\pi < x < 400 \\ A\exp\left[-\frac{(x-400)^2}{400}\right] & 400 < x < 500 \end{cases} \tag{3}$$

In the calculation, the transverse spatial resolution is 2^{13}, the transverse spatial domain is from -500 to 500 (which is taken from -80 to 80 for convenience in practice), and the step length in z-direction is 0.01. The total power is verified from 9 to 25 (which A is verified from 3 to 5). In Fig. 1, the transfer process of dark soliton is shown, which spreading $3Z_0$ (Z_0 is the diffraction length, $Z_0 = K_1\eta^2/2$). The pulse shape is well maintained. We found that the soliton pairs do not appear simultaneously when the beam enter the media. Along with the evolution of dark pulse in the media, soliton pairs appear one after another symmetrically beside the center of the hollow and evolve to the edges. For fixed intensity and as time increases, more branches appear until a steady state is reached where the number of branches is fixed. The above behaviors are same as those in Kerr media [30]. The number of branches also differs when the initial width of the input hollow is changed. With the increase of initial width, branch number increases notably. We changed the width of the input hollow, i.e., in Eq. (3), b = 1, 2, 4 and 8, respectively. The simulated results are shown in Fig. 2. It can be found that, when the initial width is large, more pairs are produced and they are closer to each other than the pairs produced with a narrow input hollow. Taking the Fig. 2b for example, the steady state of optical branching effect is shown in

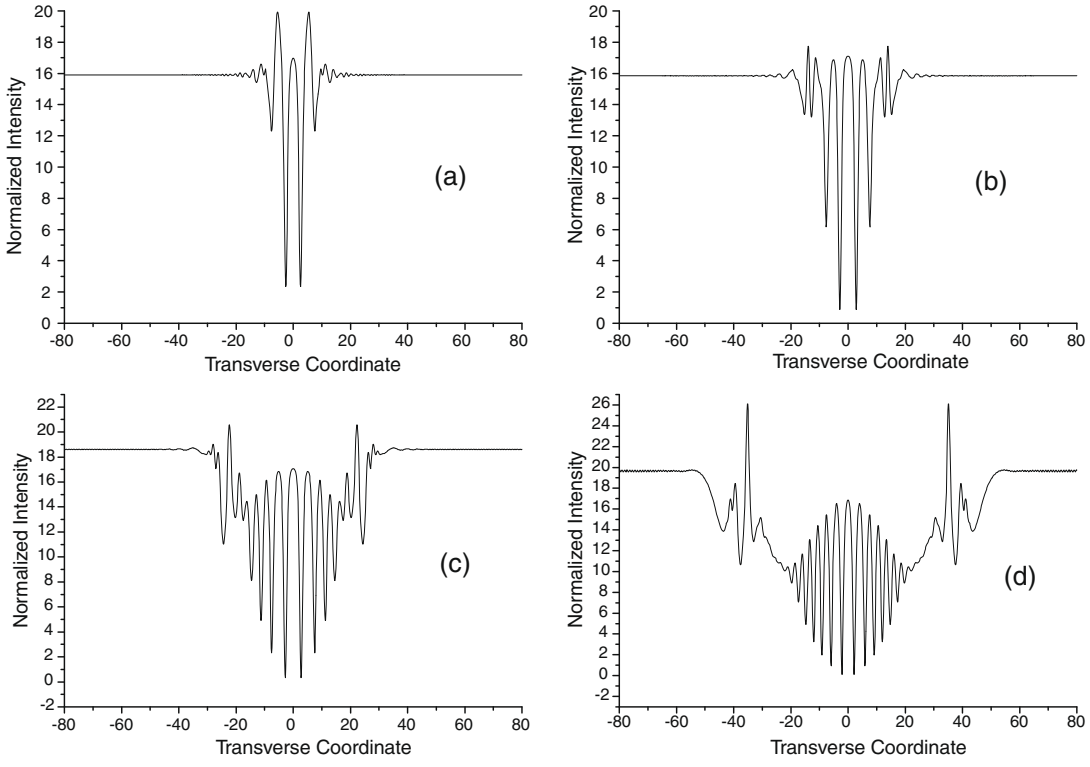

Fig. 2. The steady state of optical branching effect with the change of initial width, In Eq. (3), the parameter b is assigned as 1 (a), 2 (b), 4 (c) and 8 (d).

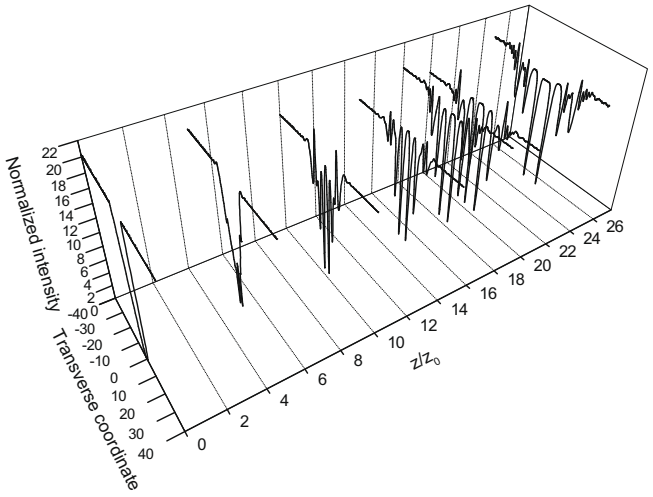

Fig. 3. The steady state of optical branching effect with $b = 2$, In Eq. (3), the value of the parameters A, β are 4.5, -15, respectively. The propagation distance z is varied from 0 to $25Z_0$.

Fig. 3. We can draw the conclusion that the dark soliton pairs have no change when the propagation distance is greater than $18Z_0$ in Fig. 3.

In nonlinear-optical fibers, the generation of temporal dark solitons in uniform background with unequal phase at $t = \pm\infty$ has been theoretically studied [31]. Dark solitons can be generated by an input pulse with a phase difference at its edges which equals π. We demonstrate that, in cascaded quadratic media, spatial dark solitons can also be generated in uniform background. A factor of $e^{(i\delta)}$ is introduced in calculation to introduce different phases. As we know, spatial dark solitons can be used to form steerable optical waveguides to be applied in all-optical apparatuses [32,33]. In cascaded media, the steerability of dark solitons by changing the phase difference at edges of the uniform background is investigated. The simulation results are shown in Fig. 4, dark solitons in uniform background is generated with different transverse velocity, depending on the phase difference δ. In Fig. 4b, when the two sides of the uniform background have a phase difference of π, a dark hollow in the center of the uniform background is generated. When the left side of the hollow has a phase of $+\frac{\pi}{2}$ ahead of the right side, the solitons hollow is generated at the left side of the center as shown in Fig. 4c. In this case, the soliton hollow sinks less than the hollow generated in the center of background, which is called grey soliton. In Fig. 4d, the left side of the hollow has a phase of $+\frac{3\pi}{2}$ ahead of the right side and the hollow is generated right to the center.

To justify the above theoretical prediction of dark spatial soliton, experimental demonstration has been implemented and the experimental setup is shown in Fig. 5. PPLN (periodically poled lithium niobate crystal) is an attractive nonlinear crystals, which can be used for SHG (Second harmonic generation), DFG (Difference frequency generation), SFG (Sun frequency generation), optical parametric oscillation, optical parametric amplification, etc. The PPLN (periodically poled lithium niobate crystal) has a period of 6.58 μm, designed for QPM frequency doubling of 1064 nm. The sample is 16 mm long and 0.5 mm thick and satisfied the requirement of good transverse homogeneity necessary for observation of spatial soliton formation. The quasi-phase-matching temperature of PPLN (periodically poled lithium niobate crystal) is about

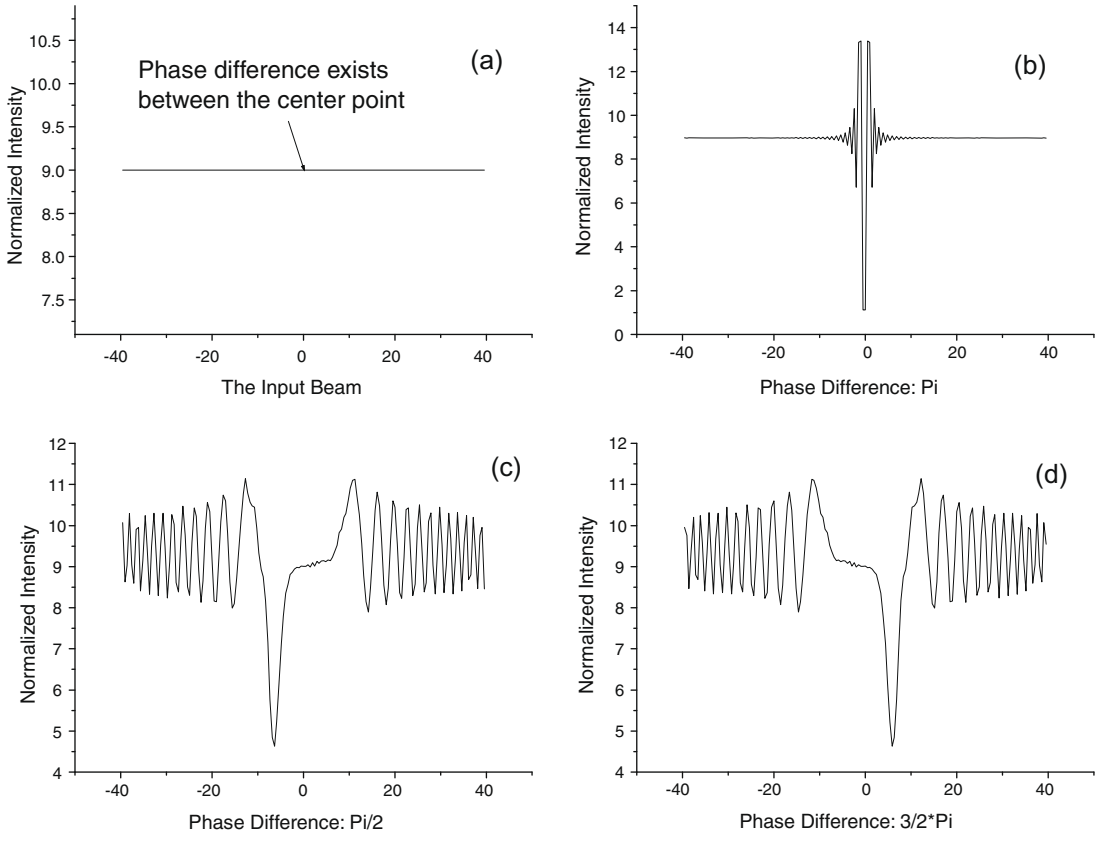

Fig. 4. Generation of dark solitons in uniform background. (a) The input uniform background; (b) hollow generated in the center of background with a phase difference of π at two edges of the uniform background; (c) hollow generated at left side of the background when left side of the hollow has a phase of $+\frac{\pi}{2}$ ahead of the right side; (d) hollow generated at right side of the background when left side of the hollow has a phase of $+\frac{3\pi}{2}$ ahead of the right side.

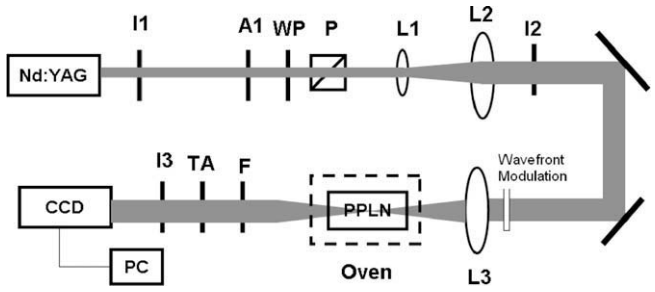

Fig. 5. General experimental setup for generation and evolution of dark spatial solitons during QPM SHG cascading process. I1–I3 iris; TA/A1:tunable attenuator/attenuator; F, wavelength filter; WP/P, waveplate/polarizer; L1/L2, 3x telescope; L3, focusing lens; a periodically poled lithium niobate (PPLN) crystal is put into an oven; a wire or a phase plate is placed in front of the L3 for wavefront modulation of the beam.

198 °C. The crystal was placed in a temperature-oven and heated to ~225 °C to ensure that not only the wave vector mismatch was negative but a quantity of wave vector mismatch was obtained. In this case wave vector mismatch Δk was about 1.2/mm. The experiments were carried out with a pulse laser that delivered 10 ns (FWHM in intensity) pulses of as much as 10 mJ of energy at 1064 nm. The beam had a Gaussian transverse profile and was polarized parallel to the c axis of the PPLN (periodically poled lithium niobate crystal) in order to use largest quadratic nonlinear coefficient, d_{33}. The beam with a diameter of about 5 mm was focused onto the entrance face of the uncoated PPLN (periodically poled lithium niobate crystal) sample to a spot of about 30 μm diameter. A magnified image of the output face of the PPLN crystal (periodically poled lithium niobate crystal) was recorded by a CCD camera connected to a personal computer. Two different filters were alternately introduced, with which either the infrared or the green output could be selected.

In this first experiment, two copper wires with the diameter of 96 μm and 175 μm are employed to mimic the initial situation in Fig. 6(c) and (d). In the simulation, the transverse spatial resolution is 2^{13}, the transverse spatial domain is from −500 to 500 (which is taken from −15 to 15 for convenience in the figures), and the step length in z-direction is 0.00658 mm. The total power is 10 mJ. The wires are put in front of the focusing lens L3. The profile of fundamental wave from the PPLN (periodically poled lithium niobate crystal) is recorded by a CCD camera. The results are shown in Fig. 6. When the narrow wire (D = 96 μm) is used, two dark lines appear in the output beam: 1st order pair of dark solitons is generated. When we change the input dark line by using the other wire (D = 175 μm), four dark lines are found in the output beam: both 1st and 2nd pairs are generated. Since the length of PPLN (periodically poled lithium niobate crystal) is determined, the only character changed in the two situations is the initial width of input dark line. This result demonstrates that the number of branches differs when the initial width of the input hollow is changed, which accord with the result of our numerical simulation based on the wave-coupling equations as shown in Fig. 6(c) and (d).

In the second experiment, a thin half-wave plate for 1064 nm with a straight cutting edge is employed to occlude the center of

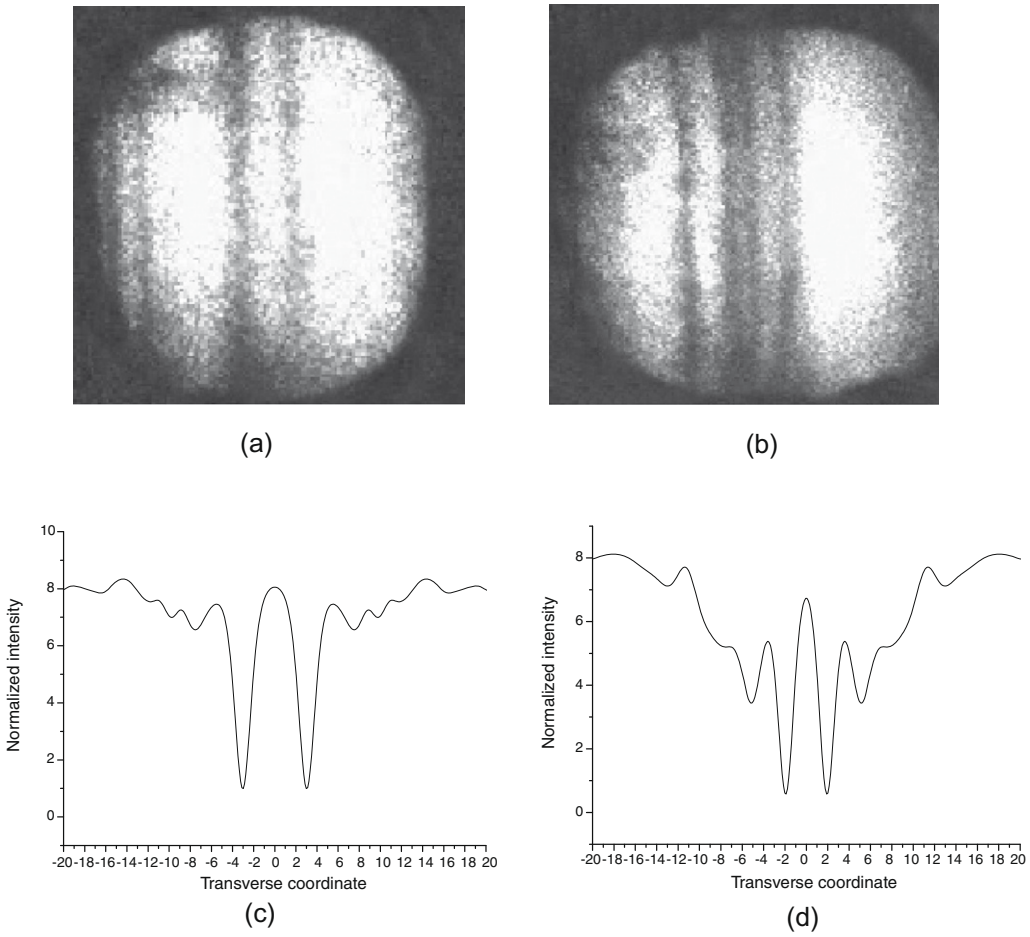

Fig. 6. (a) 1st pair of solitons generate when the diameter of wire is about 96 μm; (b) both 1st and 2nd pairs generate when the diameter of wire is about175 μm; (c) and (d) are the simulation of (a) and (b), respectively.

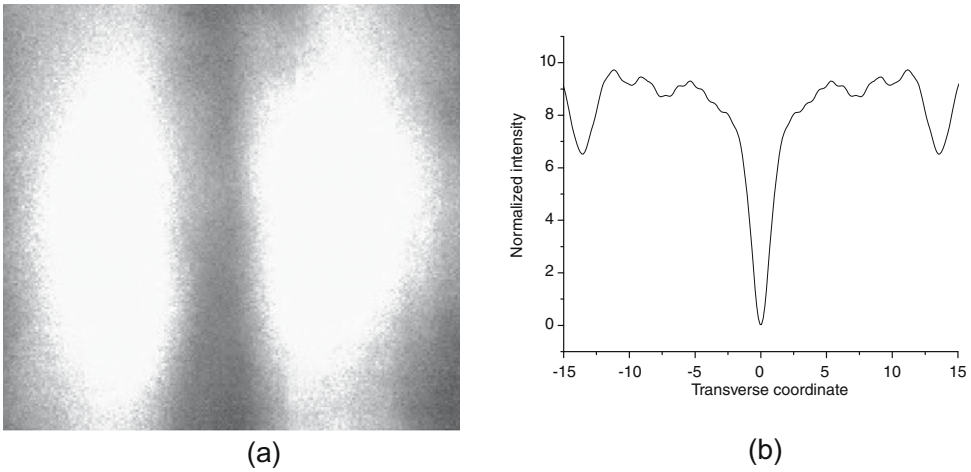

Fig. 7. (a) Image of output of fundamental wave in PPLN (periodically poled lithium niobate crystal), two sides of the beam have π-phase difference by a thin half-wave plate; (b) is the simulation of (a).

the beam. Two sides of the beam have π-phase difference. The output of the fundamental beam recorded by CCD is shown in Fig. 7(a). The result agrees well with the theoretical predictions as displayed in Fig. 7(b). To alter the phase difference, we tilt the phase plate. A little displacement of the dark hollow occurs from the center of the beam. The observation is also same as that in $\chi^{(3)}$ defocusing Kerr media.

In summary, we find out the evolution and generation of the quadratic dark spatial solitons in periodically poled lithium niobate by wavefront modulation methods. We find that the phenomena of the effect are similar to those in Kerr media. By using a wire and a phase plate, formations of spatial dark solitons are observed. Although the result presented in this *Letter* is a primary demonstration, we believe they suggest the several approaches to obtain dark spatial solitons and may have potential applications in all-optical devices, such as the block of all-optical switch circuit, dark soliton jitter [34].

Acknowledgement

It is pleasure for us to thank Professor Xianfeng Chen whom we had discussed with. This research was supported by the National Natural Science Foundation of China (No. 10734080), the National Basic Research Program 973 of China (2006CB806000), and the Shanghai Leading Academic Discipline Project (B201).

References

[1] N.N. Akhmediev, Optical and Quantum Electronics 30 (1998) 535.
[2] M. Segev, Optical and Quantum Electronics 30 (1998) 503.
[3] J.S. Aitchison, Optics Letters 15 (1990) 471.
[4] Pierre-Andre Belanger, Pierre Mathieu, Applied Optics 26 (1987) 111.
[5] G. Bartal, O. Manela, O. Cohen, J.W. Fleischer, M. Segev, Physical Review Letters 95 (2005) 053904.
[6] M. Segev, G. Stegeman, Physics Today 51 (1998) 42.
[7] G.I. Stegeman, D.N. Christodoulides, M. Segev, Optical spatial solitons: historical perspectives, Invited Paper, Special Millennium Issue of the IEEE Journal on Selected Topics in Quantum Electronics 6 (2000) 1419.
[8] A.D. Boardman, L. Pavlov, S. Tanev, Advanced Photonics with Second-order Optical Nonlinear Processes, Kluwer Academic Publishers, 1998, and reference therein.
[9] A.D. Boardman, K. Marinov, D.I. Pushkarov, A. Shivarova, Physical Review E 62 (2000) 2871.
[10] A.D. Boardman, K. Xie, Optical and Quantum Electronics 30 (1998) 783.
[11] V.E. Zakharov, A.B. Shabat, Soviet Physics JETP 34 (1972) 62.
[12] George I. Stegeman, Mordechai Segev, Science 286 (1999) 19.
[13] L.A. Ostrovskii, JETP Letters 5 (1967) 272.
[14] Yu.N. Karamzin, A.P. Sukhorukov, Soviet Physics JETP 42 (1976) 842.
[15] C.R. Menyuk, R. Schiek, L. Torner, Journal of the Optical Society of America B 11 (1994) 2434.
[16] Carl Balslev Clausen, Ole Bang, Yuri S. Kivshar, Physical Review Letters 78 (1997) 4749.
[17] Lluis Torner, Curtis R. Menyuk, William E. Torruellas, George I. Stegeman, Optics Letters 20 (1995) 13.
[18] J.F. Corney, O. Bang, Physical Review E 64 (2001) 047601.
[19] C.B. Clausen, Yu.S. Kivshar, O. Bang, P.L. Christiansen, Physical Review Letters 83 (1999) 4740.
[20] Nikola Nikolov, Dragomir Neshev, Ole Bang, Wiesław Z. Królikowski, Physical Review E 68 (2003) 036614.
[21] M. Bache, O. Bang, J. Moses, F.W. Wise, Optics Letters 32 (2007) 2490.
[22] M. Bache, O. Bang, W. Krolikowski, J. Moses, F.W. Wise, Optical Express 16 (2008) 3273.
[23] O. Bang, C.B. Clausen, P.L. Christiansen, L. Torner, Optics Letters 24 (1999) 1413.
[24] S.K. Johansen, S. Carrasco, L. Torner, O. Bang, Optics Communication 203 (2002) 393.
[25] G. Assanto, G.I. Stegeman, Optical Express 10 (2002) 388.
[26] B. Bourliaguet, V. Couderc, A. Barthelemy, G.W. Ross, P.G.R. Smith, D.C. Hanna, C. De Angelis, Optics Letters 24 (1999) 1410.
[27] H. Kim, L. Jankovic, G. Stegeman, S. Carrasco, L. Torner, D. Eger, M. Katz, Optics Letters 28 (2003) 640.
[28] P. Vidakovic, D.J. Lovering, J.A. Levenson, Optics Letters 22 (1997) 277.
[29] Wang Fei-Yu, Chen Xian-Feng, Chen Yu-Ping, Yang Yi, Xia Yu-Xing, Communications in Theoretical Physics 43 (2005) 732.
[30] D.R. Andersen, D.E. Hooton, G.A. Swartzlander, A.E. Kaplan, Optics Letters 15 (1990) 783.
[31] S.A. Gredeskul, Yu.S. Kivshar, Physical Review A 41 (1990) 3994.
[32] Barry Luther-Davies, Xiaoping Yang, Optics Letters 17 (1992) 1755.
[33] Carl Balslev Clausen, Lluis Torner, Optics Letters 24 (1999) 7.
[34] Y.S. Kivshar, B. Luther-Davies, Physics Reports 298 (1998) 81.